Journal of Colloid and Interface Science 341 (2010) 326–332

Contents lists available at ScienceDirect

Journal of Colloid and Interface Science

www.elsevier.com/locate/jcis

Droplets wetting on filament rails: Surface energy and morphology transition

Xiang-Fa Wu [a,*], Amol Bedarkar [a], K. Abraham Vaynberg [b]

[a] Department of Mechanical Engineering and Applied Mechanics, North Dakota State University, Fargo, ND 58108-6050, USA
[b] Ashland Aqualon Functional Ingredients, Wilmington, DE 19808, USA

ARTICLE INFO

Article history:
Received 6 July 2009
Accepted 11 September 2009
Available online 27 September 2009

Keywords:
Wetting and spreading
Droplets
Filament rails
Morphology transition

ABSTRACT

The morphology of liquid droplets wetting on filaments depends on the filament configuration, droplet volume, and contact angle. A stable morphology is the one that minimizes the potential energy of the droplet–filament system, while morphology transition may happen when an intermediate state exists which corresponds to a higher potential energy. This paper aims to explore such morphology transition of droplet wetting on filament rails made of two parallel identical microfilaments. Detailed numerical simulations were performed to extract the surface energy of the droplet–filament system at varying filament spacings, droplet volumes, and contact angles. Critical conditions of the morphology transition between two symmetrical wetting morphologies (i.e., liquid droplet bridge and barrel-shaped droplet) were determined. A family of characteristic curves in terms of the dimensionless droplet volume vs the filament spacing at varying contact angles was obtained, which can be used as a universal law to govern the morphology transition for such droplet–filament rail systems. The results and concepts presented in this work can be extended to broad wetting systems and utilized for the analysis and design of microfluidic devices and testers based on droplet–filament systems.

1. Introduction

Wetting and spreading of liquids on surface is a vibrant topics of science and engineering which has attracted substantial research in the past decades [1–7]. In particular, the wetting properties of liquids on microfilaments are of critical importance to the textile industry and polymer composite engineering, and even to fabrication of cosmetic products such as hair-care liquids. In the textile industry, the main concern is the nature of fiber dyeing and cleaning properties by surfactants and the ability of substances to waterproof, while in composite engineering, the wetting and spreading of polymer flows (i.e., resins) in woven and nonwoven textiles directly affect the quality and productivity of the resulting polymer composites [8,9]. Besides, in cosmetic study, it has been demonstrated that the wetting characteristics of human hair are closely related to the hair performance such as wet and dry compatibility, hair gloss and swelling properties, degree of hair damage, and the indication of the efficacy and longevity of benefiting treatment. Preferred modification of wetting properties of human hair has been considered as one of the criteria for examining the quality of particular hair-care liquids. As a matter of fact, the morphology of liquid droplets on microfilaments is dominated by the wetting property of the system, and such wetting behavior has been exploited for developing various characterization techniques for evaluating the wetting properties of liquids on surfaces, e.g., the contact angle [10].

To date, the wetting and spreading phenomena of droplets on filaments have been extensively investigated. Since the 1970s, several studies have been reported in the literature on determining the shape of a droplet wetting on a microfilament and how to accurately extract the contact angle from measurements [11–16]. Among these, Carroll [12] was the pioneer in obtaining the explicit mathematical expressions of the morphology of a barrel-shaped droplet wetting symmetrically on a cylindrical filament in terms of the combination of Legendre's elliptical functions of the first and second kinds. Several followups have been made for enhancing the accuracy of data reductions based on experimental measurements [13–16]. Besides, when considering a droplet on a microfiber, two possible droplet morphologies could be expected, i.e., the barrel- and clamshell-shaped droplets, depending on the fiber radius, droplet volume, and contact angle. McHale et al. [17] and McHale and Newton [18] have determined the critical conditions in terms of the droplet volume for the morphology transition between the barrel and the clamshell shapes of the droplet wetting on filaments at varying contact angles by using detailed numerical simulations, which were based on a surface finite element approach developed by Brakke [19]. McHale and his co-workers' numerical predictions have validated the "roll-up" condition proposed by Carroll [20] and also have been confirmed by their experiments [17,18]. Moreover, other broader studies in wetting and spreading of droplets on filaments may include droplet capturing

* Corresponding author. Fax: +1 701 231 8913.
E-mail address: Xiangfa.wu@ndsu.edu (X.-F. Wu).

0021-9797/$ - see front matter © 2009 Elsevier Inc. All rights reserved.
doi:10.1016/j.jcis.2009.09.019

on fibers and liquid films spreading and dewetting on filaments [21–25], which are particularly important to the textile industry.

However, all the studies noted above were focused on the wetting and spreading of droplets on individual filaments which excluded the interaction of neighboring filaments. In reality, fibers mostly exist in the state of yarns/bundles, fiber networks/fabrics, or woven and nonwoven textiles. Therefore, related studies would be liquid wicking in yarns [8] and wetting, spreading, and permeability of liquids in fiber textiles [5,9,26–28]. Among these, the simplest cases of wetting and spreading of liquids in aligned multifiber systems were first considered by Princen [29–31], in which asymptotic analysis was employed in determining the capillary rises in two and multiple vertical cylinders (fibers) [29,30] and the wetting lengths of droplets on two and multiple horizontal cylinders [31]. Furthermore, Keis et al. [32] recently proposed that such fiber rails made of two parallel microfibers would be potentially applicable for manipulating microquantities of fluids. In their experiments [32], the barrel-shaped droplet was placed on the fiber rails and the droplet spreading was captured by a high-speed camera. It was found in the experiments that the wicking kinetics of droplet spreading on such fiber rails roughly followed the Lucas–Washburn law [33,34]; i.e., the meniscus displacement is proportional to the complete wicking time (i.e., the time interval from the start of droplet spreading to its disappearance) for a given fiber spacing. The critical condition of droplet spreading in the fiber rail was also determined using the proposed dynamic method. Such a technique may evolve into a family of promising micro- and nanofluidic devices under development. Nevertheless, if considering a droplet wetting on such fiber rails made of two parallel identical microfilaments (cylinders) with its gravity ignored, two possible morphologies could be assumed, i.e., barrel-shaped droplet which completely wraps the two fibers (Fig. 1) and droplet bridge which only wets the side surfaces and therefore partially wraps the two fibers (Fig. 2). The transition may happen between these two possible morphologies according to the surface energy criterion at given filament radius and spacing, droplet volume, and contact angle. In the aforementioned experiments [32], the critical spreading condition is actually corresponding to the equilibrium shape (with minimum potential energy) of a droplet sitting on the fiber rails with specific spacing, while the state of wicking spreading is in accord with a nonequilibrium state. The droplet morphology with the lower surface energy is the most possible morphology to exist subjected to external perturbs, corresponding to the counterpart "roll-up" condition for a droplet wetting on a filament studied by Carroll [20] and McHale and co-workers [17,18]. Such a critical wetting condition of morphology transition is of importance to the study of droplet wetting and spreading on filament rails and relevant applications in measurements and microfluidic devices. It can be further employed for the study of microdevice assembly [35,36] and deformation and stability of fiber networks involving droplets such as the effective stiffness, collapse, and contact, among others [25,37–40].

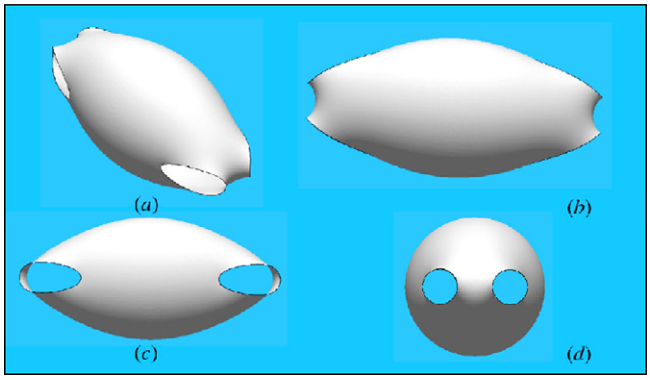

Fig. 1. Barrel-shaped droplet on filament rails made of two parallel identical microfilaments: (a) 3D view and (b–d) side views. (Filaments were not plotted; the simulation was based on the Surface Evolver [19] with filament radius $r = 1$, filament spacing $D = 2$, droplet volume $V = 400$, and contact angle: $\theta = 30°$.)

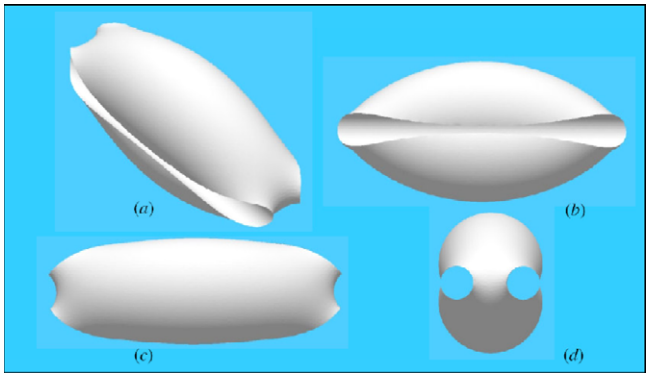

Fig. 2. Droplet bridge on filament rails made of two parallel identical microfilaments: (a) 3D view and (b–d) side views. (Filaments were not plotted; the simulation was based on the Surface Evolver [19] with filament radius $r = 1$, filament spacing $D = 2$, droplet volume $V = 400$, and contact angle $\theta = 30°$.)

Therefore, as a natural extension of the works by McHale and co-workers [17,18], in this study we performed a detailed numerical study to determine the surface energies of droplets with two different morphologies (i.e., barrel-shaped droplets and droplet bridges) at varying filament spacings, droplet volumes, and contact angles. Critical conditions of morphology transition are justified in terms of droplet volume at a given filament spacing and contact angle. A family of characteristic curves is obtained in terms of the dimensionless droplet volume vs the filament spacing ratio at varying contact angles, which can be regarded as a universal law to govern the morphology transition for a class of droplet–filament rail systems. The applications and conclusions of the study will be further addressed at the end of the paper.

2. Problem formulation and numerical simulations

In the case of a droplet wetting on filament rails made of two parallel identical microfilaments in the form of either a barrel-shaped droplet (Fig. 1) or a droplet bridge (Fig. 2), dimensional analysis [41] shows that the total surface energy of the droplet–filament system can be expressed as

$$\Pi/[(4\pi r^2)\gamma_{LV}] = f[V/(4/3\pi r^3), D/r, \theta], \tag{1}$$

where Π (Nm) is the total surface energy of the system, γ_{LV} (N/m) the surface tension of the liquid droplet (liquid–vapor interfacial tension), D (m) the filament spacing (i.e., the distance between two filament surfaces), r (m) the radius of the cylindrical filaments, θ the contact angle between the droplet and the filament, and f is a dimensionless function with respect to the dimensionless variables $V/[4/3\pi r^3]$, D/r, and θ. Herein, for the purpose of generality of the study, dimensionless expressions have been adopted in (1), where r, $4\pi r^2$, and $4/3\pi r^3$ are the reference length, area, and volume, respectively. In this investigation, the effect of gravity is excluded under the assumption of microdroplets. Therefore, in view of physics, the actual morphology of a droplet sitting on a pair of filament rails is the one which minimizes the total surface energy of the droplet–filament system. Mathematically, such morphology can be determined using two equivalent approaches. One is to solve the resulting Young–Laplace equation such that in the absence of

gravity, the equilibrium shape of a droplet is that the Laplace excess pressure, Δp, across the droplet surface is constant everywhere, i.e.,

$$\Delta p = \gamma_{LV}(1/R_1 + 1/R_2) = \text{constant}, \tag{2}$$

where R_1 and R_2 are the two principal radii of curvature at a point of the droplet surface. Equivalently, the second approach is on the basis of the minimum potential energy of the system, which is a more fundamental approach in the sense of physics. This approach addresses the equilibrium shape of a droplet, which is the one to minimize the total surface energy of the droplet–filament system such that

$$\Pi = \min[\gamma_{LV}A_{LV} + (\gamma_{SL} - \gamma_{SV})A_{SL}], \tag{3}$$

under given geometrical constraints (i.e., the constant droplet volume and geometrical constraints of filament surfaces). In relation (3), γ_{SL} and γ_{SV} are respectively the interfacial tensions of solid–liquid and solid–vapor, and A_{LV} and A_{SL} are the liquid–vapor and solid–liquid interfacial areas, respectively. In the case of a flat surface, the interfacial tensions γ_{LV}, γ_{SL}, and γ_{SV} determine the spreading power S,

$$S = \gamma_{SV} - (\gamma_{SL} + \gamma_{LV}), \tag{4}$$

and the contact angle θ,

$$\cos\theta = (\gamma_{SV} - \gamma_{SL})/\gamma_{LV}. \tag{5}$$

In relation (4), when $S > 0$, it implies that a liquid film can form at the contact angle $\theta = 0$, i.e., complete wetting on the solid surface. Based on the concept in relation (3), Wu and Dzenis [16] reformulated the governing equations of a barrel-shaped droplet on a filament and obtained all the governing equation and natural boundary conditions which validated that the apparent contact angle is independent of filament radius within the framework of classic liquid wetting and spreading theory.

Due to nonlinearity of the governing partial differential equation (PDE) (2) of wetting phenomena, only very few microdroplet shapes can be determined in explicit expressions by directly solving the PDE (2) such as a droplet sitting on a flat surface (partial sphere) and a barrel-shaped droplet on a filament by Carrol [12], among others. The determination of the morphology of droplets wetting on complex surfaces mostly relies on various skillful numerical schemes. With recent progress in computational geometry, Brakke developed the public domain finite element Surface Evolver package [19], which is demonstrated as a universal and efficient numerical tool to solve a wealth of wetting problems involving complex surface facets and multiple liquids.

Thus, in this study the Surface Evolver [19] is further utilized to calculate the surface energies of droplets wetting on filament rails for the purpose of determining the critical condition of morphology transition. Similar to that considered by McHale and co-workers [17,18], the surface energy of the droplets was used as the criterion to find the critical droplet volume at given filament spacing ratio and contact angle, at which the surface energies of a droplet bridge and a barrel-shaped droplet reach the same value.

During the numerical process, the filament radius was fixed as the reference length (unit), and the surface tension of the droplet γ_{LV} was also fixed as unit. Three contact angles $\theta = 30°$, 90°, and 120° were selected to represent liquids of three different wetting properties, i.e., hydrophilic, neutral, and hydrophobic, respectively. At each contact angle θ, five filament spacing ratios, i.e., $D/r = 1$, 2, 4, 8, and 12, were adopted, respectively. Due to the symmetry of both the droplet bridge and the barrel-shaped droplet wetting on filament rails, only 1/8 models were used for both cases in enhancing the numerical stability and computational efficiency, as illustrated in Figs. 3 and 4. In a particular simulation of the droplet wetting on the filament rails in the form of either a droplet bridge or a barrel-shaped droplet, a simple search method was employed

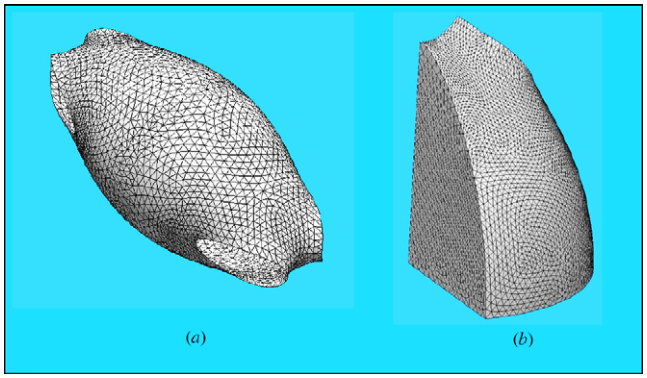

Fig. 3. Meshes used for the simulation of a barrel-shaped droplet on filament rails made of two parallel identical microfilaments: (a) full model and (b) 1/8 model (filaments were not plotted; the simulation was based on the Surface Evolver [19] with filament radius $r = 1$, filament spacing $D = 2$, droplet volume $V = 400$, and contact angle $\theta = 30°$, the actual final fine meshes are much denser and not plotted herein).

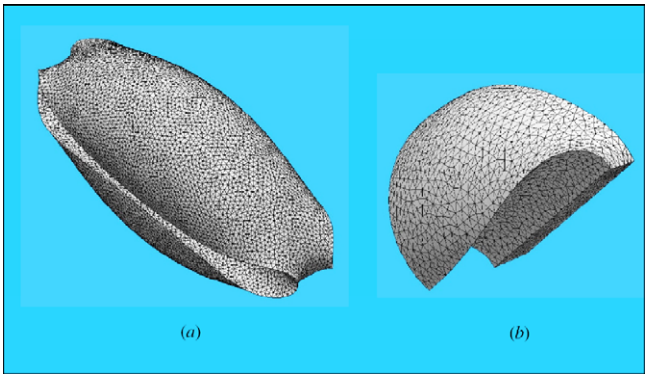

Fig. 4. Meshes used for the simulation of a droplet bridge on filament rails made of two parallel identical microfilaments: (a) full model and (b) 1/8 model (filaments were not plotted; the simulation was based on the Surface Evolver [19] with filament radius $r = 1$, filament spacing $D = 2$, droplet volume $V = 400$, and contact angle $\theta = 30°$, the actual final fine meshes are much denser and not plotted herein).

to determine the critical droplet volume at given D/r and θ. Since the numerical process of the Surface Evolver is based on numerical iteration with a very slow convergence rate at fine meshes, special care has been taken when meshing the droplet in order to accelerate the convergence rate and maintain the numerical stability during this massive simulation. The simulation was stopped when the relative numerical errors of a droplet surface energy were below 1%. Finally, all the surface energies of droplets were determined, corresponding to varying droplet volumes at given D/r and θ. After extracting the dimensionless variables with respect to the reference length r, reference area $4\pi r^2$, reference volume $4/3\pi r^3$, and reference energy $4\pi r^2\gamma$, variations of the dimensionless surface energy $\Pi/(4\pi r^2\gamma)$ vs the dimensionless droplet volume $V/(4/3\pi r^3)$ at given D/r and θ are plotted in Figs. 5–7.

3. Results and discussion

Figs. 5–7 show the numerical results of all the cases considered in the simulation. In each case, it can be observed that at given filament spacing ratio D/r and contact angle θ, the dimensionless surface energy of the droplet $\Pi/(4\pi r^2\gamma)$ grows with the increase of dimensionless droplet volume $V/(4/3\pi r^3)$ for both droplet bridge and barrel-shaped droplet. The calculated $\Pi/(4\pi r^2\gamma)$ values of the droplet bridge and barrel-shaped droplet reach the same value at

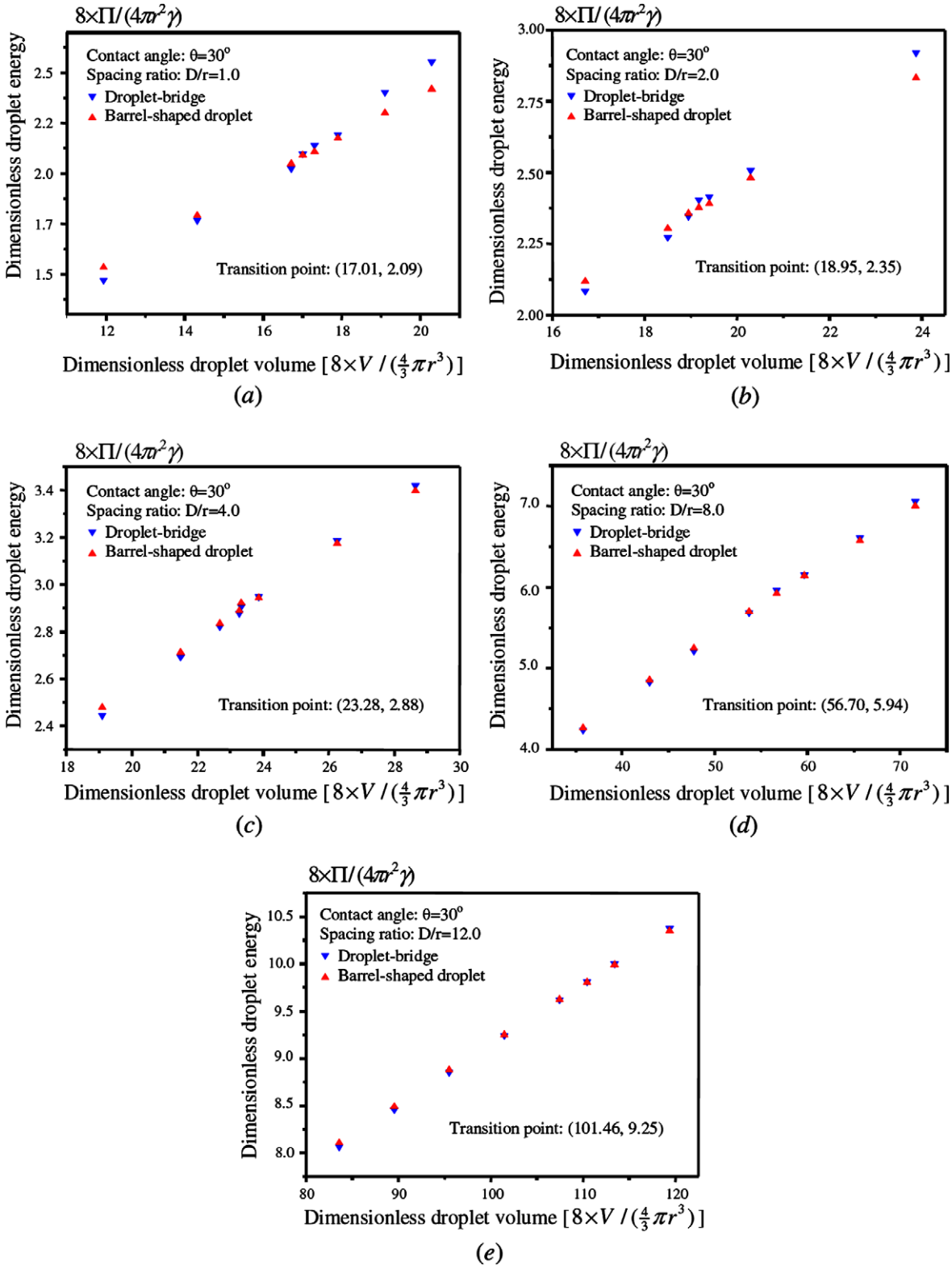

Fig. 5. Variation of the dimensionless droplet surface energy vs the dimensionless droplet volume for droplet bridges and barrel-shaped droplets at contact angle $\theta = 30°$ and varying filament spacing ratios: (a) $D/r = 1.0$, (b) $D/r = 2.0$, (c) $D/r = 4.0$, (d) $D/r = 8.0$, and (e) $D/r = 12.0$.

a critical droplet volume V_0 (with $4/3\pi r^3$ as the reference volume). When the droplet volume is below V_0, the surface energy of a droplet bridge is lower than that of a barrel-shaped droplet with the same volume. This means that the morphology of a droplet bridge is a more stable morphology compared to its counterpart barrel-shaped droplet of the same volume. In contrast, once the droplet volume passes over the critical volume V_0, the surface energy of a barrel-shaped droplet is lower than that of a droplet bridge of the same volume. In this case, the barrel-shaped droplet is a more stable morphology. As a result, the critical droplet volume V_0 determines the transition point of droplet morphology between a droplet bridge and a barrel-shaped droplet.

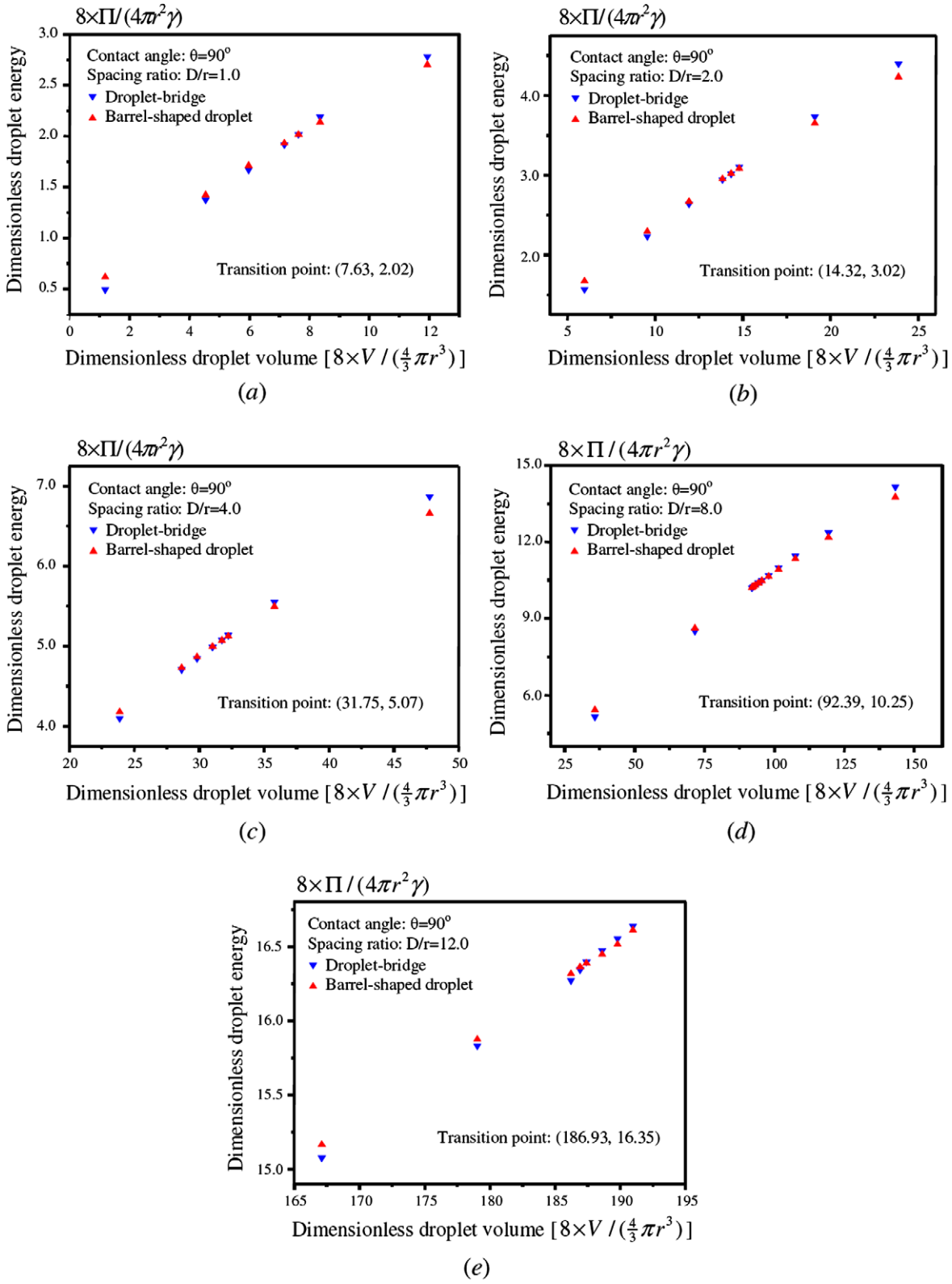

Fig. 6. Variation of the dimensionless droplet surface energy vs the dimensionless droplet volume for droplet bridges and barrel-shaped droplets at contact angle $\theta = 90^\circ$ and varying filament spacing ratios: (a) $D/r = 1.0$, (b) $D/r = 2.0$, (c) $D/r = 4.0$, (d) $D/r = 8.0$, and (e) $D/r = 12.0$.

Furthermore, for a droplet–filament rail system made of a symmetrically wetting droplet on two parallel identical filaments, the critical volume V_0 is a dimensionless function with respect to the filament spacing ratio D/r and contact angle θ:

$$V_0 = W(D/r, \theta). \tag{6}$$

Based on the numerical results obtained in this simulation, a family of W curves is plotted in Fig. 8, each of which divides the $(D/r, V_0)$ domain into two subdomains at given contact angle θ, i.e., the upper barrel-shaped droplet domain and the lower droplet-bridge domain. It can be observed from Fig. 8 that the critical droplet volume V_0 increases rapidly with the increase of either

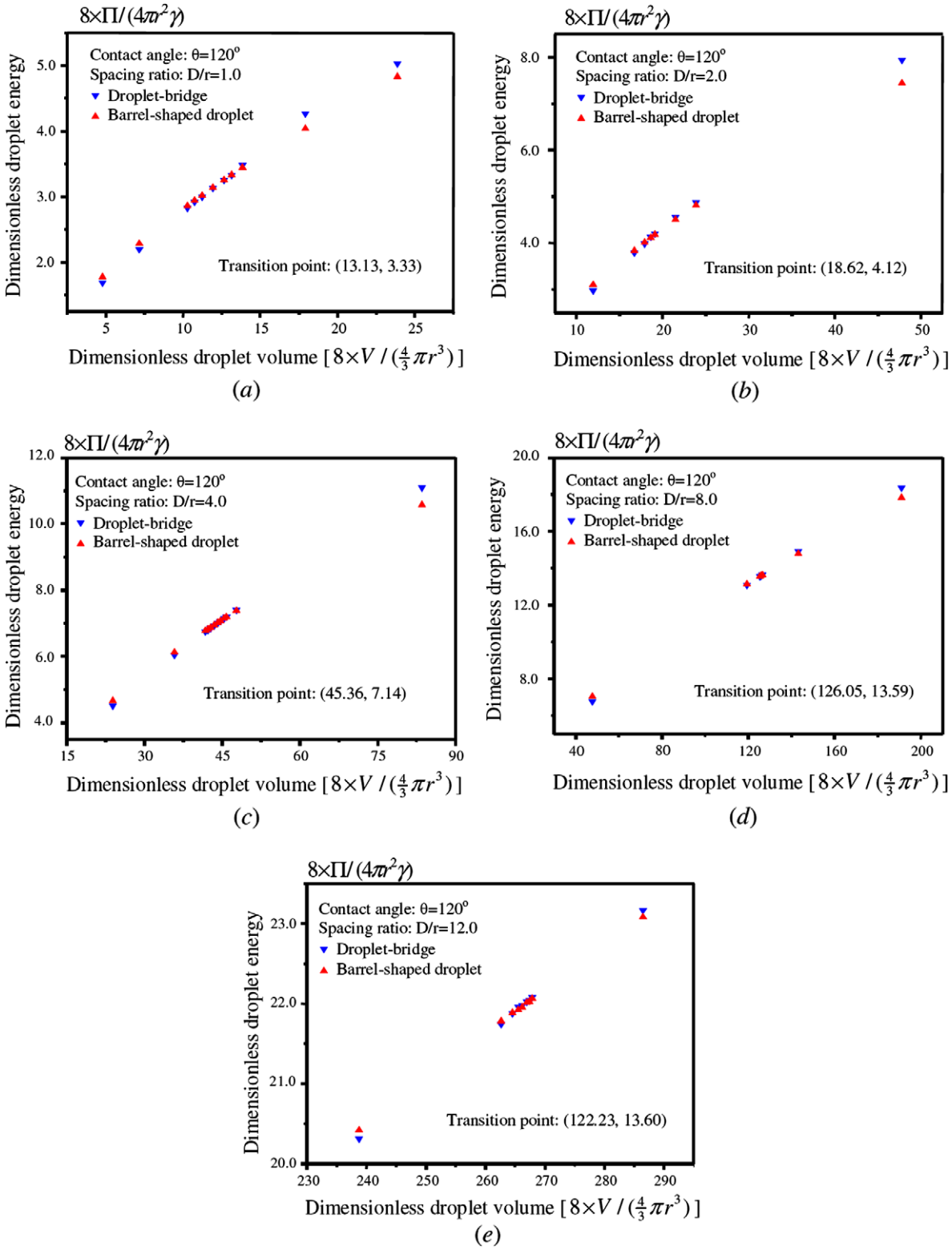

Fig. 7. Variation of the dimensionless droplet surface energy vs the dimensionless droplet volume for droplet bridges and barrel-shaped droplets at contact angle $\theta = 120°$ and varying filament spacing ratios: (a) $D/r = 1.0$, (b) $D/r = 2.0$, (c) $D/r = 4.0$, (d) $D/r = 8.0$, and (e) $D/r = 12.0$.

the filament spacing ratio D/r or the contact angle θ at relatively large filament spacing ratio D/r (>3). Therefore, a liquid with a higher hydrophobicity to the filament material has a larger critical transition volume V_0. However, at relatively small filament spacing ratio D/r (<2), the W curves are overlapped in Fig. 8. This implies that at small D/r, droplet bridges of hydrophilic liquids ($\theta < 90°$) can assume a more stable morphology compared to that of neutral and hydrophobic liquids with the same droplet volume. This is because the capillary force of a hydrophilic droplet on a pair of filament rails at lower D/r yields a much larger wetting length than

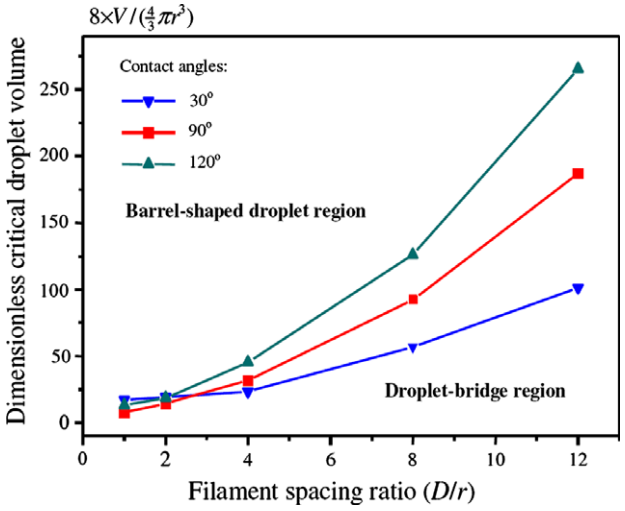

Fig. 8. Variations of the dimensionless critical droplet volume (V_0) for morphology transition vs the filament spacing ratio (D/r) at three contact angles $\theta = 30°$, 90°, and 120°. Each wetting characteristic curve (W curve) divides the (D/r, V_0) domain into the upper barrel-shaped droplet region and the lower droplet-bridge region.

that of more hydrophobic liquids with larger contact angle θ as discussed by Princen [29–31], and therefore reduces the height of the droplet to spill over the filaments. Furthermore, when considering the delivery of microquantities of liquids by using filament rails, the filament spacing should be smaller, comparable to the filament diameter as demonstrated by Keis et al. [32]. In such case, the wicking spreading of the droplet happens and the morphology of the droplet becomes more complicated. Theoretically, the final equilibrium state can be determined by the present simulation, while large quantities of the droplet volume compared to the characteristic length (filament spacing) may substantially complicate the process.

Consequently, a wetting state on the W curve corresponds to a neutral state at which the morphology transition of the droplet may happen nearby the W curve. Therefore, the W curves are the wetting characteristic curves which govern the morphology transition of droplets wetting on filament rails. Clearly, such characteristic W curves are of critical importance to the application of microfilament rails for the study of wetting and spreading of droplets in textiles and the design of microfluidic devices for various applications [35,36]. One such application would be the delivery of micro- and nanoliquids through filament rails as demonstrated by Keis et al. [32]. As one of the outcomes, the present study has determined the upper limit of the liquid volume that can be delivered through liquid bridges on a filament rail. The experimental determination of such a critical condition is still open. Methodologically, the dynamic method demonstrated by Keis et al. [32] could be used for this purposes.

4. Concluding remarks

In this study the morphology transition between liquid droplet bridges and barrel-shaped droplet wetting on filament rails has been studied through a detailed numerical simulation at varying filament spacings, droplet volumes, and contact angles. A family of wetting characteristic curves (W curves) has been determined in terms of dimensionless critical droplet volume V_0 vs the filament spacing ratio D/r at varying contact angle θ. These W curves can be considered as a universal law of droplets wetting on filament rails at given contact angles. For a fixed contact angle, each characteristic W curve divides the (D/r, V_0) phase space into two regions, i.e., the upper barrel-shaped droplet region corresponding to large volume droplets and the lower droplet-bridge region corresponding to small volume droplets. By varying the filament spacing ratio D/r and contact angle θ, the wetting characteristic W curves for broader D/r and θ can be determined. The results and concepts obtained in this study can be used for the analysis and design of microfluidic devices and testers based on droplet–filament rail systems and can be also extended to other boarder wetting systems.

Acknowledgment

The authors thank one of reviewers for pointing out the important Ref. [32].

References

[1] P.G. de Gennes, Rev. Mod. Phys. 57 (1985) 827.
[2] P.G. de Gennes, F. Brochard-Wyart, D. Quere, Capillarity and Wetting Phenomena—Drops, Bubbles, Pearls, Waves (Translated by A. Reisinger), Springer, New York, 2004.
[3] V.M. Starov, M.G. Velarde, C.J. Radke, Wetting and Spreading Dynamics, CRC Press, Boca Raton, FL, 2007.
[4] D. Bonn, J. Eggers, J. Indekeu, J. Meunier, E. Rolley, Rev. Mod. Phys. 81 (2009) 739.
[5] M. Alava, M. Dube, M. Rost, Adv. Phys. 53 (2004) 83.
[6] D. Quere, Annu. Rev. Mater. Res. 38 (2008) 71.
[7] A.W. Adamson, A.P. Gast, Physical Chemistry of Surfaces, sixth ed., Wiley, New York, 1997.
[8] X.M. Chen, K.G. Kornev, Y.K. Kamath, A.V. Neimark, Text. Res. J. 71 (2001) 862.
[9] D. Lukas, N. Pan, Polym. Compos. 24 (2003) 314.
[10] N.R. Demarquette, Int. Mater. Rev. 48 (2003) 247.
[11] J.I. Yamaki, Y. Katayama, J. Appl. Polym. Sci. 19 (1975) 2897.
[12] B.J. Carroll, J. Colloid Interface Sci. 57 (1976) 488.
[13] H.D. Wagner, J. Appl. Phys. 67 (1990) 1352.
[14] T. Ogawa, M. Ikeda, J. Adhes. 43 (1993) 69.
[15] B.H. Song, A. Bismarck, R. Tahhan, J. Springer, J. Colloid Interface Sci. 197 (1998) 68.
[16] X.F. Wu, Y.A. Dzenis, Acta Mech. 185 (2006) 215.
[17] G. McHale, M.I. Newton, B.J. Carroll, Oil Gas Sci. Technol. 56 (2001) 47.
[18] G. McHale, M.I. Newton, Colloids Surf., A 206 (2002) 79.
[19] K.A. Brakke, Surface Evolver, 2000. <www.susqu.edu/facstaff/b/vrajjer/evolver>.
[20] B.G. Carroll, Langmuir 2 (1986) 248.
[21] E. Lorenceau, C. Clanet, D. Quere, J. Colloid Interface Sci. 279 (2004) 192.
[22] Z.B. Huang, X.M. Liao, Y.Q. Kang, G.F. Yin, Y.D. Yao, J. Colloid Interface Sci. 330 (2009) 399.
[23] D. Quere, Annu. Rev. Fluid Mech. 31 (1999) 347.
[24] A.L. Yarin, A. Oron, R. Rosenau, Phys. Fluids A 5 (1993) 91.
[25] A.L. Yarin, G.G. Chase, W. Liu, S.V. Doiphode, D.H. Reneker, AIChE J. 52 (2006) 217.
[26] A. Koponen, D. Kandhai, E. Hellen, M. Alava, A. Hoekstra, M. Kataja, K. Niskanen, P. Sloot, J. Timonen, Phys. Rev. Lett. 98 (1998) 716.
[27] E. Rodriguez, F. Giacomelli, A. Vazquez, J. Compos. Mater. 38 (2004) 259.
[28] T.S. Lundstrom, V. Frishfelds, A. Jakovics, J. Compos. Mater. 38 (2004) 1137.
[29] H.M. Princen, J. Colloid Interface Sci. 30 (1969) 69.
[30] H. M Princen, J. Colloid Interface Sci. 30 (1969) 359.
[31] H. M Princen, J. Colloid Interface Sci. 34 (1970) 171.
[32] K. Keis, K.G. Kornev, A.V. Neimark, Y.K. Kamath, in: S. Guceri, Y.G. Gogotsi, V. Kuznetov (Eds.), Nanoengineered Nanofibrous Materials, Springer, Verlag, 2004, p. 173.
[33] R. Lucas, Kollid Z. 23 (1918) 15.
[34] E.W. Washburn, Phys. Rev. 17 (1921) 273.
[35] R.R.A. Syms, J. Microelectromech. Syst. 8 (1999) 448.
[36] R.R.A. Syms, E.M. Yeatman, V.M. Bright, G.M. Whitesides, J. Microelectromech. Syst. 12 (2003) 387.
[37] X.F. Wu, Y.A. Dzenis, Nanotechnology 18 (2007) 285702.
[38] X.F. Wu, Y.A. Dzenis, J. Phys. D 40 (2007) 4296.
[39] X.F. Wu, Y.A. Dzenis, J. Appl. Phys. 98 (2005) 093501.
[40] X.F. Wu, Y.A. Dzenis, J. Appl. Phys. 102 (2007) 044306.
[41] J.D. Logan, Applied Mathematics, second ed., Wiley, New York, 1997.